# Intramolecular Co-reaction Accelerated Electrochemiluminescence of Polypeptide-biomineralized Gold Nanoclusters for Targeted Detection of Biomarkers

Yue Jia[†,#], Shanghua Liu[‡,#], Yu Du[†], Lei Yang[†], Xuejing Liu[†], Lei Liu[†], Xiang Ren[†,*], Qin Wei[†,*], Huangxian Ju[†,§]

[†] *Collaborative Innovation Center for Green Chemical Manufacturing and Accurate Detection, Key Laboratory of Interfacial Reaction & Sensing Analysis in Universities of Shandong, School of Chemistry and Chemical Engineering, University of Jinan, Jinan 250022, P. R. China*

[‡] *School of Chemistry and Chemical Engineering, Shandong University of Technology, Zibo, 255049, P. R. China*

[§] *State Key Laboratory of Analytical Chemistry for Life Science, Department of Chemistry, Nanjing University, Nanjing 210023, China*

***Corresponding Authors**

E-mail: chem_renx@163.com (X. R.); sdjndxwq@163.com (Q.W.)

## Contents:

## S1.Materials and Reagents

$H_2N$-MMYYHFRRHL-COOH (MYH-10) is purchased from Apeptide Co. Ltd. (Shanghai, China). CYFRA21-1 and its antibody are purchased from Shanghai Linc-Bio Science Co. Ltd. (Shanghai, China). $HAuCl_4 \cdot 4H_2O$ is purchased from Sigma-Aldrich (Beijing, China). Phosphate-buffered saline (PBS) (1/10 M) is prepared by mixing the stock solutions of 1/10 M $Na_2HPO_3$ and 1/10 M $KH_2PO_3$ with different proportions. NaOH, $FeCl_3$, urea, tris(3-aminoethyl)amine (TAEA), mercaptoacetic acid (TGA) and 1-(3-Dimethylaminopropyl)-3-ethylcarbodiimide hydrochloride (EDC) are purchased from Macklin Reagent Co. Ltd. All the other reagents in the experiments are analytical grade and used without further purification.

## S2.Apparatus

Electrochemical experiments are performed on RST electrochemical workstation (Zhengzhou Shiruisi Instrument Technology Co. Ltd, China). The ECL detections are carried out with MPI-1 ECL analyzer (Xi'an Remax Electronic Science & Technology Co. Ltd, China). Reversed-phase high performance liquid chromatogram (RP-HPLC, Agilent, America) equipped with a BioCore SEC-300 column (4.6 × 300 mm, 5 μm, China). In order to characterize the $Fe_2O_3$ and Au NCs, high resolution transmission electron microscope (HRTEM, JEOL-JEM-2100F, Japan), scanning electron microscope (SEM, Oxford, England), X-ray diffraction (XRD, D8 focus diffractometer, Bruker AXS, Germany), circular dichroism spectrum (CD, America), laser particle analyzer(LPSA, NKT-N9, China) are used.

**S3. RP-HPLC analysis for MYH-10 evaluation**

The detection of anti-CYFRA21-1 is achieved by an Agilent reverse phase high-performance liquid chromatography (RP-HPLC) system equipped with a BioCore SEC-300 column (4.6 × 300 mm, 5 μm) and a diode array detector. 5 μL of different concentrations of anti-CYFRA21-1 are injected into a sample loop. The six-port valve is switched to the "inject" state, and the targets are eluted into the column for separation with the HPLC mobile phase (water/acetonitrile, 90:10, v/v). Then, the targets are further detected at a wavelength of 280 nm with a diode array detector. Additionally, the flow rate of the mobile phase is 0.35 mL $min^{-1}$.

**S4.ECL detection of purposed biosensor**

The biosensors are measured utilizing a RST electrochemical workstation as excitation source and a MPI-I weak-light detection system as ECL signal collector. The three-electrode system is composed of a working electrode (purposed biosensor), a counter electrode (platinum wire) and a reference electrode (Ag/AgCl electrode). The cyclic voltammetry (CV) potential is set from 0.3 to 1.2 V with an appropriate scan rate of 0.15 V $s^{-1}$. The ECL signals are released in 10 mL of PBS (1/10 M, pH 7.8) without anything else and enlarged by a photomultiplier, of which the potential of is set at 600 V and amplification level was adjusted to Ⅲ.

**S5. EIS characterization of stepwise biosensor fabrication**

Stepwise characterization of the proposed biosensor is confirmed with electrochemical impedance spectroscopy (EIS) in 5 mM $K_3[Fe(CN)_6]$ containing 0.1 M KCl. Impedance spectra of ITO at different modified steps are shown in Figure S1. $Fe_2O_3$ NAs-shrouded ITO (red curve) showed a smaller semicircle compared with bare ITO (black curve) because of the increment of electro-active surface area. After the continuous to modify of a lamina of nonconductive *a*-Au NCs on the ITO surface, resistance (blue curve) increased slightly, which benefit by the good conductivity of small molecular weight polypeptide template Au NCs. After the final modification of antibody and its antigen, the resistance further increased observably (pink and green curves).

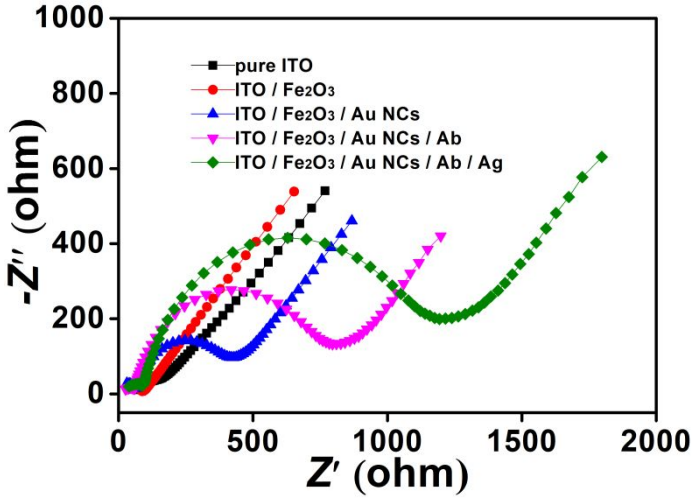


**Figure S1**. EIS profiles of stepwise-modified electrodes in 10 mL of PBS (pH 7.8, 0.1 M) containing 0.1 M KCl and 5 mM $K_3[Fe(CN)_6]$.

**S6 Characterization of successful carboxylation of $Fe_2O_3$**

To characterize the successful carboxylation of $Fe_2O_3$. The fourier transform infrared spectroscopy (FTIR) is used to explore the functional groups changes of $Fe_2O_3$ surface. As can be seen from Figure S2, the pure $Fe_2O_3$ have no obvious FTIR absorption (green curve). After functionalization with TGA, the obtained product had many additional characteristic peaks compared with the original sample (pink line). The wide absorption peaks in the range of 2500 ~ 3300 $cm^{-1}$ belong to the stretching vibration of O-H. This kind of band broadening of the very strong O-H bands is quite typical in solid-state samples, and can hide superimposed bands like the weaker C-H stretching mode. The absorption peaks at 1250 $cm^{-1}$ and 1430 $cm^{-1}$ represent the deformation vibration of O-H. It is worth noting that the sharp absorption peak at 1714 $cm^{-1}$ corresponds to the double-bond stretching vibration peak of C=O.[1-4]

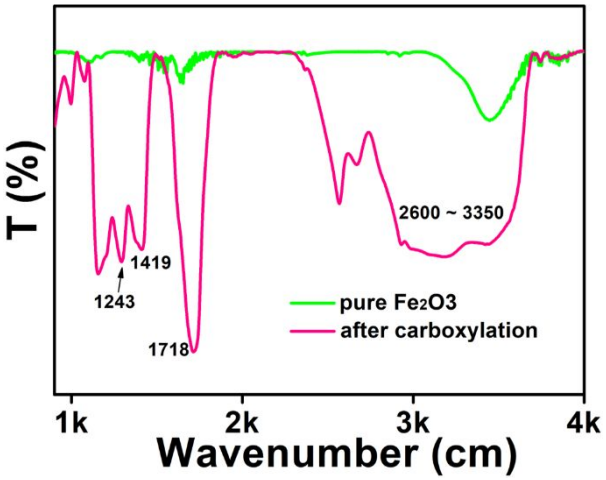


**Figure S2.** FTIR spectra of ITO/$Fe_2O_3$ (green curve) and carboxylic ITO/$Fe_2O_3$ (pink curve).

**S7 Optimal conditions of the ECL system**

As a novel ECL system, the optimal ECL conditions should be explored, which could enhance the ECL efficiency and maintain the immune molecules with active states. First and foremost, the optimal pH value of the Au NCs/TAEA system is explored in a series of PBS with different pH range from 5.0 to 8.15, and the results are presented in Figure S3a. It has been clearly seen that a drastic increase of ECL signal occurred when the pH value improved from 5.0 to 7.8, which could be explained by abundant $OH^-$ accelerating the ECL process of to produce more Au high-energy-state Au $NCs^*$. The ECL intensity still increase slightly when pH is over 7.8, but 7.8 is chosen as the optimal pH for CYFRA21-1 detection owing to excessive pH could cause protein metamorphosis. Then, the $Fe_2O_3$ on ECL enhancement is explored by adjusting the calcination time of $Fe_2O_3$ from 1 h to 5 h. As shown in Figure S3b, $Fe_2O_3$ may not be able to form an ordered arrays structure within short time calcination, but when the time is more than 2 h, the density region of the array structure is stable, resulting in a stable ECL enhancement. Furthermore, the dosage of TAEA and Au NCs are also closely related to the ECL intensity (Figure S3c and d), which are involved in the ECL process. Trace amounts of TAEA and Au NCs would result in an incomplete process of protonation and insufficient high-energy-state Au $NCs^*$. But superfluous TAEA can actuate the reverse reaction in the ECL process, as well as limited by the active area of the electrode, the fixation capacity of Au NCs cannot increase indefinitely, and the peptide encapsulated on the surface will decrease the electron transfer efficiency as a result. Therefore, when the amount of Au NCs increases, the intensity of ECL will decrease moderately.

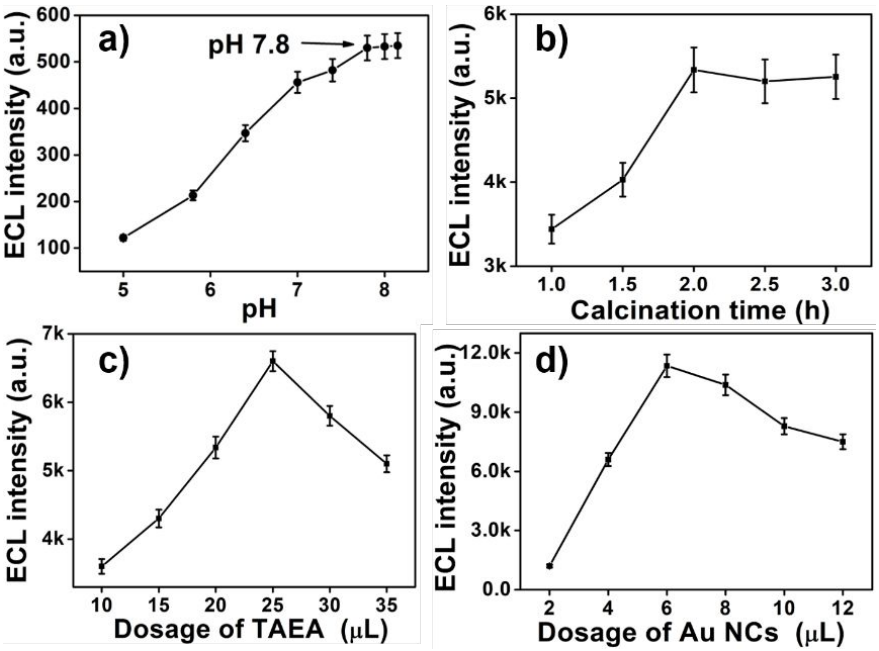


**Figure S3.** Effect of different pH of PBS (a), calcination time of $Fe_2O_3$ (b), dosage of TAEA (c) and dosage of Au NCs (d) on ECL intensity. Error bars = SD, ($n$ = 3).

**S8 Repeatability tests of the biosensor**

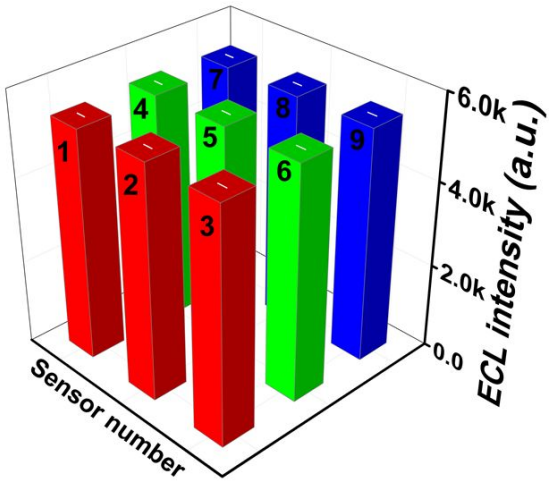


**Figure S4.** Repeatability of the biosensor with nine electrodes incubated with 1 pg $mL^{-1}$ CYFRA21-1. Error bars = SD, ($n$ = 3).

## REFERENCES

1. Nhlapo, N. S.; Focke, W. W.; Vuorinen, E., TGA-FTIR study of the vapors released by triethylamine-acetic acid mixtures. *Thermochim. Acta* **2012,** *546*, 113-119.

2. Li, J. S.; Wang, H.; Guo, Z. K.; Wang, Y. G.; Ma, H. M.; Ren, X.; Du, B.; Wei, Q., A "turn-off" fluorescent biosensor for the detection of mercury (II) based on graphite carbon nitride. *Talanta* **2017,** *162*, 46-51.

3. Saber-Samandari, S.; Saber-Samandari, S.; Joneidi-Yekta, H.; Mohseni, M., Adsorption of anionic and cationic dyes from aqueous solution using gelatin-based magnetic nanocomposite beads comprising carboxylic acid functionalized carbon nanotube. *Chem. Eng. J.* **2017,** *308*, 1133-1144.

4. Klepper, K. B.; Nilsen, O.; Hansen, P. A.; Fjellvag, H., Atomic layer deposition of organic-inorganic hybrid materials based on saturated linear carboxylic acids. *Dalton Trans.* **2011,** *40* (17), 4636-4646.